**INTERNATIONAL JOURNAL OF OPTIMIZATION IN CIVIL ENGINEERING**
***Int. J. Optim. Civil Eng., 2018; 8(2):311-328***

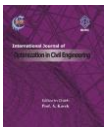

# DIFFERENT NEURAL NETWORKS AND MODAL TREE METHOD FOR PREDICTING ULTIMATE BEARING CAPACITY OF PILES

H. Harandizadeh[1*, †], M. M. Toufigh[1] and V. Toufigh[2]
[1]*Department of Civil Engineering, Shahid Bahonar University of Kerman, 22 Bahman Blvd., Kerman, P.O.BOX: 76169133, Iran*
[2]*Department of Civil Engineering, Graduate University of Advanced Technology, Kerman, P.O.BOX: 76315117, Iran*

## ABSTRACT

The prediction of the ultimate bearing capacity of the pile under axial load is one of the important issues for many researches in the field of geotechnical engineering. In recent years, the use of computational intelligence techniques such as different methods of artificial neural network has been developed in terms of physical and numerical modeling aspects. In this study, a database of 100 prefabricated steel and concrete piles is available from existing publications to solve issues related to pile's bearing capacity analysis. Three different artificial neural network algorithms were developed for comparing and verifying the obtained results at analyzing the bearing capacity of pile in soils. During the modeling process, the geometric properties of different piles, soil materials properties, friction angle and flap numbers (hammer blows) were selected as input parameters to the selected network and the output from the network was considered as the bearing capacity of the pile. Finally, the performance of radial base function type neural networks was compared with model tree method and predictive neural networks based on different learning algorithms such as Levenberg-Marquardt and Bayesian Regulation Back Propagation Algorithms. It was observed that the radial base neural network in some cases achieved better results from accuracy based on common statistical parameters such as correlation coefficient, mean absolute error percentage and root mean square error as compared to other stated methods and it showed the acceptable performance in modeling and predicting the desired output close to the target's results.

**Keywords:** Pile Bearing Capacity, Deep Foundation, RBF Type Neural Network, Model Tree, Levenberg Marquardt Learning Algorithm, Bayesian Regulation Learning Algorithm, Multilayer Perceptron Neural Network

[*]Corresponding author: Department of Civil Engineering, Shahid Bahonar University of Kerman, 22 Bahman Blvd., Kerman, P.O.BOX: 76169133, Iran
[†]E-mail address: hoomanharandizadeh@eng.uk.ac.ir (H. Harandizadeh)

Received: 23 June 2017; Accepted: 2 September 2017



## 1. INTRODUCTION

Various methods and efforts have been made to determine the amount of ultimate bearing capacity of deep foundation. The result of these researches is the presentation of formulas, solutions or diagrams based on empirical methods of using plastic theory or numerical methods. The disadvantage of semi-experimental methods and the method of plastic theory in estimating the bearing capacity of deep foundation is the use of simplifying assumptions which in most cases leads to a conservative estimate of the bearing capacity. Most of these methods are set for homogeneous soil conditions or maximum two layers, which is not compatible with the actual conditions of deep foundation.

Calculating the bearing capacity of deep foundation which are in layered soils has a more complicated process than homogeneous or double-layered substrates. One of the reasons for such complexities is the difference in the behavior of these soils against loading due to the increase in the number of effective parameters on the bearing capacity compared to homogeneous soils. In this paper, estimating the bearing capacity of deep foundation using numerical modeling and artificial neural network technique has been investigated. Many recent studies have been limited to develop numerical models in explaining the behavior of foundations on layered soil based on element method.

Many researchers have investigated about the bearing capacity of piles and have achieved various methods and formulas. Most of the methods estimate the bearing capacity approximately by the mechanical parameters of the soil and the geometric characteristics of the pile. Goh has used the length and diameter of the pile, the average effective stress, the non-drain shear strength as network inputs and frictional surface strength as network outputs to predict the bearing capacity of the pile [1]. The obtained results of the network by Semple method, Rigden method and α method were compared and it was determined that the neural network offers better responses in comparison with test and older methods. Also, Goh [2] predicted the bearing capacity of slamming pile through the neural network. The used data were the results of actual loading experiments on steel and concrete piles that were screwed into sandy soils. When the model was evaluated by the test setup, it was seen that the network is well able to model the bearing capacity of the pile. By measuring the synaptic weights (connecting weights), it was determined that the main input factors are the weight and type of hammer [1,2]. Lee and Lee [3] for the first time have predicted the bearing capacity of pile using artificial neural networks. In his research, he used neural network back propagation errors to predict the bearing capacity of the piles and was consistent with the results of other experiments. The results indicate that the maximum error did not exceed 25%. Teh et al. [4] provided a network for estimating the static capacity of the pile calculated by dynamic stress wave data for square-shaped piles made of prefabricated concrete. The neural network fully absorbed the training data set and was able to predict the ultimate capacity of the pile with a square average error of less than 0.0003 {Formatting Citation}. Abu Kiefa [5] presented three models of the neural network (GRNNM3, GRNNM2, GRNNM1) to determine the capacity of slamming pile in non-adhesive soils. The first model was used to estimate the total bearing capacity of the pile, the second model

was used to estimate the capacity of the pile tip and the third model was used to estimate the lateral capacity of the pile. The obtained results of this study were compared with four methods of (Meyerhof), (Coyle and Castello), American Petroleum Institute (API) and (Randolph). The predicted results provided 0.95 for the Coefficient of Correlation by neural networks while this number for the four methods mentioned above was in the range of 0.52 and 0.63 [5]. Hanna et al. [6] used the neural network to determine the efficiency of the pile group in non-cohesive soils. Several static indicators such as R, MAE, RMSE and average percentage error were calculated to evaluate the accuracy of the developed model. The mentioned values for R (0.85), MAE (0.157), RMSE (0.232) and average percent error (13%) indicate that the used neural network model had a high accuracy. Shahin et al. [6] briefly outlined the application of artificial neural network in geotechnical engineering as well as the accuracy of the neural network and the power of some artificial neural networks [7, 8, 9]. Kordjezi and Pooyanejad [10] have used a machine learning method called support vector machine (SVM) to predict the ultimate bearing capacity of piles under the influence of axial load. Maizir and Kassin [11] used the collected data from approximately 300 projects in Indonesia and Malaysia for training and testing of artificial neural networks to predict the axial bearing capacity of the slamming piles for the various pile characteristics and the results of the slamming pile data analysis (PDA). McVay et al. [12] searched on pile / shaft design using an artificial neural network by genetic algorithm method (Genetic programming) using Florida data and information based on the bearing capacity of the piles (the wall and tip resistance of the pile), the internal friction angle (ø) and the extraction SPT number of boreholes. Also, a lot of researches has been done on the application of artificial intelligence algorithms [13,14] in other civil engineering fields (structural and geotechnical engineering) in order to predict the parameters and optimizing earth, marine and space structures. Kaveh et al. examined the optimization of structures by neural networks based on the descending gradient learning algorithm [15]. In this study, a neural computing strategy was developed to combine neural network information processing capabilities and structural numerical optimization. In this strategy, an improved anti-imitation neural network was used. Two artificial neural networks, one for constraints and another for constraint gradients were trained and structural optimization was performed using these networks [16,17]. Kaveh and Servati [18] evaluated the application of various neural networks for analyzing and designing spatial structures used in existing buildings. Kaveh and Iranmanesh [17] performed a comprehensive review of propagation neural networks and counter propagation neural networks in the analysis and optimization of structures. Kaveh and Servati [18] have been successfully performed the design of two-layer networks in spatial structures due to the complexity and timing of calculations in analyzing and designing these structures using backpropagation neural networks. Kaveh et al. [19] used BP neural networks for prediction of moment-rotation characteristic for semi-rigid connections.Kaveh and Raiessi Dehkordi [20] investigated some researches using BF and RBF neural networks for the analysis and design of structural domes.

## 2. METHODS AND ASSUMPTION

The research method consists of three parts. In the first part of this study, there are the soil

characteristics and the geometric properties of the pile obtained from the results of loading pile test that were collected from published articles in some regions of Iran and regions of different parts of the world. In the second part, computational artificial intelligence techniques in geotechnical engineering related to the estimation of ultimate bearing capacity were developed using radial network of neural function type, multi-layer perceptron propagation algorithm and model tree. MATLAB was used in modeling and performing current algorithms. In the third part of this study, input data into the neural network was presented and optimized. Neural network architecture was trained to achieve the desired goal. Neural network performance compared with each other about common statistical parameters and finally the efficiency and performance of different models of artificial neural network and model tree in calculating the ultimate pile capacity analysis was evaluated. The range, precision and uniformity of the input data are very significant in achieving the output results desired from the ANN model which is close to the actual values of the target. Generally, an artificial neural network is a model that uses empirical data to create a logical relationship between inputs and output data. Due to some collection limitations in this field and empirical experiments, the existing published articles were used as referral materials. In this study, input data were selected as geometric characteristics of the pile and soil layers resistance parameters. The output of the numerical modeling network was considered as the bearing capacity of the pile. The structure of the neural network system as well as the type of transfer functions and the number of neurons in each layer using test and error to create linear or nonlinear logical relationship between the input parameters of the network (effective input variable) and the output parameter (target candle bearing capacity) and The efficiency and reliability of the network were evaluated based on the correlation coefficient and the network error was measured between the target value and the network output.

## 3. SOIL AND PILE INFORMATION

A database of 100 prefabricated concrete and steel piles was collected from existing papers and publications. Geometric characteristics of the pile, mechanical properties of the soil, number of flaps (number of hammer blows) and hammer blow energy for each individual pile and also static loading test results for each pile were collected. Soil drainage cohesion, drained soil friction angle and effective soil specific weight are variables that describe the soil conditions. The cross-section area of the pile and the embedded length of pile are the variables that describe the geometric properties of the pile. In addition to the variables mentioned, the Flap number was used to determine all the effective hidden parameters in calculating the bearing capacity of the pile. Seven variables were considered to predict the bearing capacity of the pile:

A = cross-sectional area of the pile ($m^2$)

C'= drained soil cohesion (KN / $m^2$)

Number of Flap = multiplication of the number of hammer blows (N) in the relative energy of the hammer ($E_r$) for penetration of the pile in last one meter

L = the length of the embedded pile in the soil

$\gamma'$ = Effective and specific weight of soil (KN / $m^3$)

$\delta$ = Angle of friction between soil and pile (°)

$\phi$ = internal friction angle of drained soil (°)

Soil information, friction angle between various materials, collected data, the number of Flap from driving the piles, the static loading test results and the specific location of each test are shown in Table 1 and 2 respectively.

Table 1: Friction angles between various materials and various soils or rocks [16]

| **Interface materials** | **Friction angle δ, degrees** |
|---|---|
| Clean fine sand, silty or clayey fine to medium sand | ϕ |
| Clean fine to medium sand, silty medium to coarse sand, silty or clayey gravel | ϕ |
| Clean gravel, gravel-sand mixture, well-graded rock fill with spall | 22° |
| Clean gravel, gravel-sand mixture, well-graded rock fill with spall | 22°-26° |
| Clean gravel, gravel-sand mixtures, coarse sand | ϕ |
| Clean sand, silty sand-gravel mixture, single-size hard rock fill | 17° |
| Clean sand, silty sand-gravel mixture, single-size hard rock fill | 17°-22° |
| Clean sound rock | 35° |
| Dressed hard rock on dressed hard rock | 29° |
| Dressed hard rock on dressed soft rock | 33° |
| Dressed soft rock on dressed soft rock | 35° |
| Fine sandy silt, non-plastic silt | ϕ |
| Fine sandy silt, non-plastic silt | 11° |
| Fine sandy silt, non-plastic silt | 14° |
| Formed concrete or concrete sheet piling against the following: | |
| Masonry on wood (cross grain) | 26° |
| Mass concrete or masonry on the following: | |
| Medium stiff and stiff clay and silty clay | ϕ |
| Silty sand, gravel or sand mixed with silt or clay | 14° |
| Silty sand, gravel, or sand mixed with silt or clay | 17° |
| Steel on steel at sheet pile interlocks | 17° |
| Steel sheet piles against the following: | |
| Various structural materials: | |
| Very stiff and hard residual or pre-consolidated clay | ϕ |
| Wood on soil | 14°-16° |

Table 2: Database of 100 ultimate pile bearing capacities for different hammer strike, pile geometry, and soil properties characteristics [21]

| Pile No. | Location | Pile Materials | Cohesion (kN/m2 | Friction Angle (°) | Soil Specific Weight (kN/m3) | Pile-Soil Friction Angle (°) | Flap Number | Pile Area (m2) | Pile Length (m) | Pile Capacity (kN) |
|---|---|---|---|---|---|---|---|---|---|---|
| 1 | Haraz-Iran | Steel | 33 | 28.85 | 9.82 | 12.49 | 20.1 | 0.1 | 19.5 | 1040 |
| 2 | | Steel | 33 | 29.89 | 9.73 | 12.41 | 27 | 0.1 | 23.5 | 1400 |
| 3 | | Steel | 33 | 28.81 | 9.82 | 12.49 | 20 | 0.1 | 19.4 | 990 |
| 4 | | Steel | 0 | 28 | 9.57 | 12.27 | 21 | 0.1 | 19.5 | 960 |
| 5 | | Steel | 0 | 28 | 9.69 | 12.22 | 24 | 0.1 | 23.5 | 1330 |
| 6 | | Steel | 63 | 5 | 9.69 | 11.2 | 40 | 0.1 | 19.4 | 1230 |
| 7 | Mahshahr-Iran | Concrete | 6.37 | 29.84 | 9.7 | 14 | 177 | 0.16 | 25.3 | 3335 |
| 8 | | Concrete | 6.8 | 29.3 | 9.92 | 14 | 61 | 0.16 | 21.5 | 2000 |

| Pile No. | Location | Pile Materials | Cohesion (kN/m2 | Friction Angle (°) | Soil Specific Weight (kN/m3) | Pile-Soil Friction Angle (°) | Flap Number | Pile Area (m2) | Pile Length (m) | Pile Capacity (kN) |
|---|---|---|---|---|---|---|---|---|---|---|
| 9 | | Concrete | 6.4 | 29.78 | 9.73 | 14 | 180 | 0.16 | 24.9 | 3142 |
| 10 | | Concrete | 7 | 29 | 10.03 | 14 | 80 | 0.16 | 19.9 | 2520 |
| 11 | | Concrete | 6.64 | 29.48 | 9.84 | 14 | 115 | 0.16 | 22.7 | 2840 |
| 12 | | Concrete | 6.4 | 29.8 | 9.72 | 14 | 250 | 0.16 | 25 | 3867 |
| 13 | | Concrete | 6.34 | 29.87 | 9.69 | 14 | 202 | 0.16 | 25.6 | 4012 |
| 14 | | Concrete | 6.65 | 29.46 | 9.85 | 14 | 69 | 0.16 | 22.6 | 2278 |
| 15 | | Concrete | 7 | 29 | 10.34 | 14 | 50 | 0.16 | 15.2 | 1900 |
| 16 | | Concrete | 138 | 4.23 | 7.52 | 14 | 246 | 0.16 | 22.9 | 2500 |
| 17 | Mahshahr-Iran | Concrete | 142 | 4.14 | 7.55 | 14 | 210 | 0.16 | 23.4 | 2250 |
| 18 | | Concrete | 148 | 4.03 | 7.58 | 14 | 306 | 0.16 | 24 | 2700 |
| 19 | Gulf of Mexico | Steel | 8.7 | 24 | 8.55 | 11.75 | 790 | 0.89 | 61 | 19000 |
| 20 | (Stockard, | Steel | 7.72 | 26.04 | 9.54 | 12.84 | 632 | 0.89 | 82 | 24900 |
| 21 | | Steel | 1.4 | 29.39 | 9.1 | 13.75 | 1360 | 1.59 | 98 | 48470 |
| 22 | India (Stockard, | Steel | 1.58 | 27.67 | 8.66 | 12.68 | 1300 | 1.17 | 98 | 36250 |
| 23 | 1986) | Steel | 4.87 | 26.77 | 8.81 | 12.1 | 2130 | 1.59 | 98 | 52100 |
| 24 | | Steel | 2.76 | 28.39 | 8.93 | 13.12 | 1750 | 1.59 | 90 | 49350 |
| 25 | | Steel | 7.47 | 35.99 | 12.91 | 16.68 | 178 | 0.1 | 18 | 5900 |
| 26 | | Steel | 6.59 | 35.64 | 12.92 | 16.13 | 178 | 0.1 | 20.4 | 6200 |
| 27 | | Steel | 6.71 | 35.69 | 12.92 | 16.2 | 180 | 0.1 | 20 | 6120 |
| 28 | Alton-Illinois | Steel | 7.78 | 36.62 | 13.19 | 17 | 86 | 0.1 | 16.1 | 4280 |
| 29 | (Larry, 1988) | Steel | 7.78 | 36.62 | 13.15 | 17 | 70 | 0.1 | 16.4 | 3130 |
| 30 | | Steel | 7.83 | 36.56 | 13.49 | 17 | 29 | 0.07 | 14.2 | 1321 |
| 31 | | Steel | 7.83 | 36.57 | 13.46 | 17 | 63 | 0.1 | 14.4 | 1300 |
| 32 | | Steel | 7.79 | 36.6 | 13.27 | 17 | 49 | 0.13 | 15.6 | 1830 |
| 33 | Illinois | Steel | 14.6 | 32.22 | 9.89 | 13.75 | 16 | 0.16 | 15.2 | 1043 |
| 34 | (Fellenius, | Steel | 14.6 | 32.22 | 9.89 | 13.75 | 15 | 0.1 | 15.2 | 987 |
| 35 | | Concrete | 51.4 | 0 | 11.19 | 14 | 361 | 0.16 | 24.5 | 2030 |
| 36 | Bandar Imam-Iran | Concrete | 26 | 0 | 11.68 | 14 | 110 | 0.16 | 16 | 1145 |
| 37 | | Concrete | 54.8 | 0 | 11.15 | 14 | 482 | 0.16 | 25.9 | 2250 |
| 38 | | Concrete | 0.07 | 22.43 | 11.33 | 15.45 | 328 | 0.16 | 25.5 | 2600 |
| 39 | | Concrete | 0.06 | 23.79 | 11.26 | 15.51 | 202 | 0.16 | 28.5 | 2200 |
| 40 | | Concrete | 51.8 | 11.81 | 7.3 | 14.88 | 234 | 0.16 | 26.5 | 2920 |
| 41 | Bandar Imam-Iran | Concrete | 51 | 12.24 | 7.36 | 15.02 | 263 | 0.16 | 27.2 | 2880 |
| 42 | | Concrete | 58.6 | 11.43 | 8.34 | 14.59 | 112 | 0.16 | 14.5 | 680 |
| 43 | | Concrete | 58.5 | 11.38 | 8.29 | 14.58 | 78 | 0.16 | 14.7 | 540 |
| 44 | | Concrete | 136 | 27.82 | 8.94 | 14 | 167 | 0.16 | 18.2 | 2100 |
| 45 | Shiraz-Iran | Concrete | 137 | 27.1 | 8.84 | 14 | 94 | 0.16 | 19.5 | 1700 |
| 46 | | Concrete | 138 | 29.3 | 9.21 | 14 | 98 | 0.16 | 15.9 | 2200 |
| 47 | Ontario | Steel | 18.2 | 20 | 5.45 | 13.75 | 78 | 0.09 | 60 | 2750 |
| 48 | (Fellenius and | Steel | 17.9 | 19.76 | 5.43 | 13.82 | 87 | 0.09 | 62 | 2870 |
| 49 | Altaee, 2002) | Steel | 17 | 18.93 | − 5−.38 | 14.07 | 96 | 0.09 | 70 | 3050 |
| 50 | Bandar Abbas- | Steel | 45.8 | 31.11 | 11.23 | 10.14 | 406 | 0.78 | 20.5 | 2670 |
| 51 | | Steel | 49.8 | 31.01 | 11.2 | 12.47 | 670 | 1.16 | 22.5 | 3350 |
| 52 | | Steel | 45.8 | 31.11 | 11.23 | 10.14 | 730 | 0.78 | 20.5 | 3750 |
| 53 | | Steel | 45.8 | 31.11 | 11.23 | 10.14 | 1236 | 0.78 | 20.5 | 4100 |
| 54 | | Steel | 45.8 | 31.11 | 11.23 | 10.14 | 710 | 0.78 | 20.5 | 3450 |
| 55 | | Steel | 45.2 | 31.12 | 11.23 | 12.63 | 756 | 0.78 | 20.2 | 3570 |

| Pile No. | Location | Pile Materials | Cohesion (kN/m2 | Friction Angle (°) | Soil Specific Weight (kN/m3) | Pile-Soil Friction Angle (°) | Flap Number | Pile Area (m2) | Pile Length (m) | Pile Capacity (kN) |
|---|---|---|---|---|---|---|---|---|---|---|
| 56 | | Steel | 48.8 | 31.03 | 11.21 | 12.5 | 1030 | 1.16 | 22 | 3570 |
| 57 | | Steel | 44.7 | 31.14 | 11.24 | 12.65 | 1463 | 1.16 | 20 | 4936 |
| 58 | | Steel | 51.5 | 30.97 | 11.2 | 12.4 | 1448 | 1.16 | 23.5 | 4900 |
| 59 | | Steel | 49.8 | 31.01 | 11.2 | 12.47 | 1298 | 1.16 | 22.5 | 4650 |
| 60 | | Steel | 41.1 | 31.23 | 11.25 | 12.78 | 1610 | 1.16 | 18.5 | 2150 |
| 61 | | Steel | 42.4 | 31.2 | 11.24 | 12.74 | 1590 | 1.16 | 19 | 4150 |
| 62 | | Steel | 45.8 | 31.11 | 11.23 | 10.14 | 701 | 0.89 | 20.5 | 3600 |
| 63 | | Steel | 44.7 | 31.14 | 11.24 | 12.65 | 1112 | 0.89 | 20 | 4000 |
| 64 | | Steel | 49.8 | 31.01 | 11.2 | 12.47 | 990 | 1.16 | 22.5 | 3870 |
| 65 | Bandar Imam- | Concrete | 8.21 | 25.02 | 9.045 | 12.295 | 510 | 0.89 | 71.5 | 21965 |
| 66 | | Concrete | 6.58 | 29.57 | 9.81 | 14 | 65 | 0.16 | 23.4 | 2682.5 |
| 67 | | Concrete | 6.7 | 29.39 | 9.88 | 14 | 72 | 0.16 | 22.4 | 2846 |
| 68 | | Concrete | 6.52 | 29.64 | 9.78 | 14 | 97 | 0.16 | 23.8 | 3368.5 |
| 69 | | Concrete | 7.03 | 35.815 | 12.915 | 16.405 | 423 | 0.1 | 19.2 | 6065 |
| 70 | | Concrete | 6.49 | 29.665 | 9.77 | 14 | 70 | 0.16 | 24.1 | 3160 |
| 71 | | Concrete | 8.59 | 16.615 | 8.93 | 14 | 113 | 0.16 | 19 | 2215 |
| 72 | | Concrete | 9.2 | 4.083 | 7.565 | 14 | 186 | 0.16 | 23.7 | 2490 |
| 73 | | Concrete | 7.24 | 36.155 | 13.055 | 16.6 | 321 | 0.1 | 18.1 | 5215 |
| 74 | | Concrete | 7.8 | 36.59 | 13.32 | 17 | 116 | 0.08 | 15.3 | 2240.5 |
| 75 | | Concrete | 7.81 | 36.585 | 13.365 | 17 | 132 | 0.11 | 15 | 1580 |
| 76 | Mahshahr-Iran | Steel | 24.6 | 32.22 | 9.89 | 13.75 | 56 | 0.13 | 15.2 | 1030 |
| 77 | | Steel | 33.7 | 0 | 11.432 | 14 | 306 | 0.16 | 20.2 | 1602.5 |
| 78 | | Steel | 27.4 | 11.215 | 11.24 | 14.725 | 505 | 0.16 | 25.7 | 2440 |
| 79 | | Steel | 21.49 | 28.53 | 8.88 | 13.215 | 1106 | 1.38 | 32.2 | 4275 |
| 80 | | Steel | 23.81 | 27.58 | 8.8715 | 12.61 | 1323 | 1.59 | 36.5 | 5740 |
| 81 | | Steel | 25.9 | 17.8 | 9.28 | 15.195 | 196 | 0.16 | 27.5 | 2575 |
| 82 | | Steel | 27.4 | 19.6 | 8.615 | 14.29 | 153 | 0.16 | 16.4 | 1335 |
| 83 | Isfahan-Iran | Concrete | 38 | 28.2 | 9.025 | 14 | 196 | 0.16 | 23.7 | 1965 |
| 84 | | Concrete | 28.1 | 19.88 | 5.44 | 13.785 | 70 | 0.09 | 27 | 2825 |
| 85 | | Concrete | 31.4 | 25.02 | 8.305 | 12.105 | 725 | 0.44 | 25 | 2875 |
| 86 | | Concrete | 45.8 | 31.11 | 11.23 | 10.14 | 2291 | 0.78 | 35.5 | 3790 |
| 87 | | Concrete | 54.8 | 11.835 | 7.85 | 14.805 | 123 | 0.16 | 37.8 | 1795 |
| 88 | Bandar Abbas- | Steel | 47.8 | 31.06 | 11.215 | 11.305 | 1631 | 0.97 | 21.5 | 3565 |
| 89 | | Steel | 47 | 31.075 | 11.22 | 12.565 | 2078 | 0.97 | 21.1 | 3585 |
| 90 | | Steel | 48.1 | 31.055 | 11.217 | 12.525 | 2147 | 1.16 | 21.7 | 3870 |
| 91 | | Steel | 45.4 | 31.12 | 10.967 | 12.625 | 2243 | 1.16 | 20.5 | 3415 |
| 92 | | Steel | 44.1 | 31.155 | 11.235 | 11.44 | 1009 | 1.02 | 19.7 | 5465 |
| 93 | | Steel | 49.8 | 31.01 | 11.2 | 12.47 | 849 | 1.16 | 22.5 | 4275 |
| 94 | | Steel | 31.1 | 34.42 | 11.54 | 15.375 | 131 | 0.1 | 15.7 | 2648.5 |
| 95 | | Steel | 29.6 | 18.31 | 12.17 | 15.5 | 291 | 0.13 | 20.4 | 2595 |
| 96 | Isfahan-Iran | Concrete | 33 | 29.37 | 9.775 | 12.45 | 14 | 0.1 | 21.5 | 1235 |
| 97 | | Concrete | 28.5 | 28.405 | 9.695 | 12.38 | 14 | 0.1 | 19.4 | 1145 |
| 98 | | Concrete | 31.5 | 16.5 | − 9−.69 | 11.71 | 22 | 0.1 | 21.4 | 1295 |
| 99 | | Concrete | 26.9 | 18.28 | 12.582 | 15.5 | 131 | 0.11 | 15.1 | 1248 |
| 100 | | Concrete | 31.3 | 18.285 | 12.305 | 15.5 | 320 | 0.13 | 20.1 | 1790 |

## 4. BASIC CONCEPTS

### *4.1 Framework of MLP and RBF neural networks*

An artificial neural network is formed of input, hidden and output layers, hence it is known as a three-layer network. The input layer contains independent variables that are attached to the hidden layer for processing. The hidden layer contains activation functions and calculates the weight of the variables in order to explore the predictive effects on the target variables. In the output layer, the process of forecasting or classification ends and the results are presented with the estimation of a small error. Generally, a back propagation algorithm trains a predictive neural network. In the training sessions, the back propagation algorithm learns the relationship between the specified set of input and output pairs. The back propagation training algorithm acts as follows: First, it propagates the input values forward to the hidden layers, and then back propagates the resulting sensitivities in order to make smaller errors. At the end, the calculation process updates the weights. The mathematical framework of the back propagation algorithm is seen in numerous studies such as "Feed forward network training with Marquardt algorithm".

In ANNs, some techniques are used with the back propagation training algorithm to obtain a small error. This makes the network response smoother and less likely to over fit for the training patterns. However, the back-propagation algorithm has a slow convergence and may cause over fitting issues. Back-propagation algorithms that can be synchronized faster are developed to overcome the convergence problem. Similarly, some legal methods have been developed to solve over fitting issues in artificial neural networks. Among the tuning techniques, Levenberg-Marquardt (LM) and Bayesian regularization (BR) can obtain lower mean square errors than other existing algorithms for the function approximation problems. LM was developed especially for faster convergence in back-propagation algorithms. Basically, the BR training algorithm has a goal function that includes the sum of the remaining squares and the sum of square weights to minimize the estimated errors and to achieve a well- generalized model.

Basically, the multi-layer perceptron artificial neural network (MLPANN) or radial basis function artificial neural network (RBFANN) algorithms can be investigated instead of BR or LM. However, it is known that BR and LM algorithms perform better than conventional methods (MLPNN, RBFNN) in terms of speed and over fitting issues in some cases.

In this research, the performance of various multi-layer predictive neural network learning algorithms such as feedforward Bayesian regulation (BR) learning algorithm and feedforward Levenberg-Marquardt (LM) algorithm were compared with the radial basis function neural network (RBFNN) and model tree (MT) algorithms. To compare the efficiency of the mentioned algorithms, commonly statistical indices such as correlation coefficient and mean square error between actual values (target values) and predicted values (expected output value) were used using RBFNN, BR, LM and MT algorithms to evaluate the performance of developed models.

The neural network models used in our research (MLP and RBF) are able to solve any function approximation. Creating a neural model involves determining the proper neural network structure with the number of layers and the number of neurons in each layer, as well as the training algorithm. The extensive experiment of the research results of the MLP and RBF architecture is shown in Figs. 1 and 2 respectively. The MLP neural network model

(Fig. 1) consists of two input layers, two hidden and one output layer. The input is for both models. The coordinates are access point and the receiving points while the output is normalized field strength. The output of the MLP model can be expressed using the equation below:

$$P_r = \varphi_0\left(\sum_{k=1}^{K} w_{ok}\left(\varphi_{h2}\left(\sum_{j=0}^{M} w_{kj} v_j\left(\varphi_{h1}\left(\sum_{i=0}^{N} w_{ji} u_i\right)\right)\right)\right)\right) \quad (1)$$

Explanation of the above equation:

- $w_{ok}$ shows the synaptic weight with the K-neuron in the hidden layer to the single-output neuron
- $v_j$ represents the j-th vector element that enters the second hidden layer
- $w_{kj}$ is binding weights between the neurons of two hidden layers
- $u_i$ represents the I-th element of the input vector, which consists of the appropriate coordinates (x, y, z)
- $w_{ji}$ is the binding weight between the neurons of the first hidden layer and inputs
- $\varphi_{h1}$, $\varphi_{h2}$ and $\varphi_o$ are the activation functions of the neurons from the first and second hidden layer and the output layer respectively.

The activation function is of the sigmoid type in the hidden layers while a simple linear function is used in the output layer. In this research, we select two training algorithms for training the neural network: MLP network with two different algorithms such as BP Levenberg Marquardt and BP Bayesian Regulation which converge faster than the standard BP algorithm that was taught. This is an approximation algorithm of the Newton method which has a stronger optimization technique than the descending gradient method.

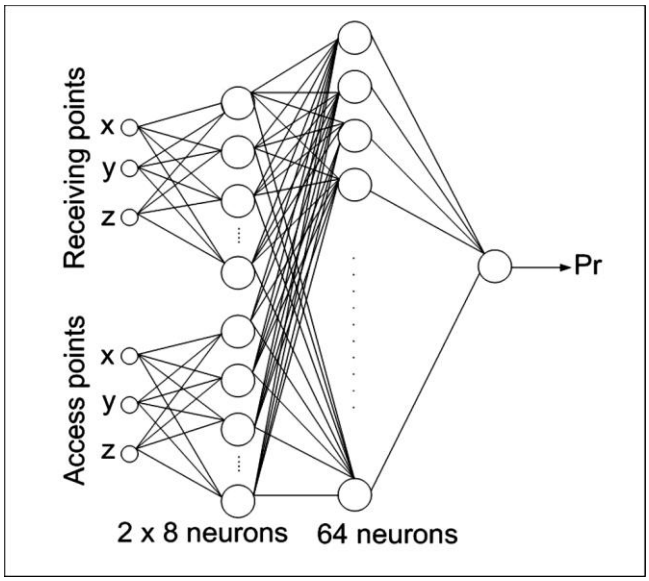


Figure 1. Multilayer perceptron neural network structure

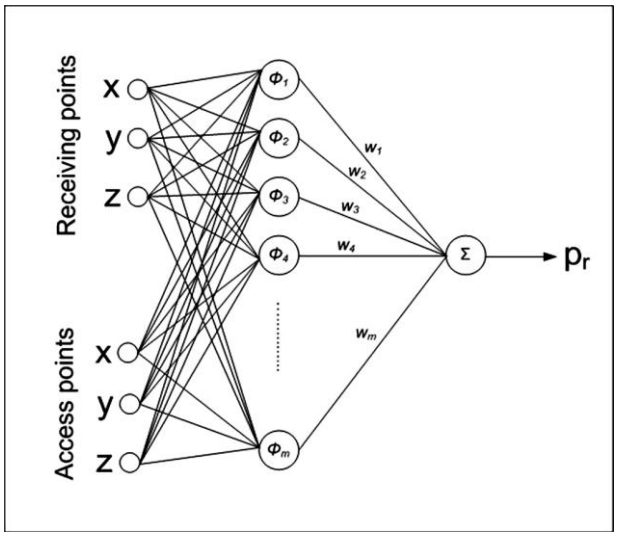


Figure 2. RBF neural network structure

The RBF neural network (Fig. 2) contains an input layer, a hidden layer, and a neuron in the output layer. The inputs are represented by the coordinates of the access point and the receiving points. The hidden layer conducts the convert and transfer on data from the input space to the hidden space. The linear output layer creates the field strength for the proper input coordinates. The output of the RBF neural network is computed as below:

$$P_r = \sum_{i=1}^{M} w_i \phi_i(u, c_i) = \sum_{i=1}^{M} w_i \phi_i \left( \left\| u - c_i \right\|_2 \right) \qquad (2)$$

Where $u$ is the input vector (coordinates of the access point and receiving points), $\phi_i$ is a function of the set of all positive real numbers, ||. || shows that Euclidean distance and $w_i$ represents the weights in the output layer, $M$ denotes the number of neurons in hidden layer and $c_i$ is as the RBF centers in the output vector space. The $\phi_i$ function is a Gaussian multivariable function which is defined by the below equation:

$$\phi(u, c_i) = e^{-\frac{1}{2\sigma_i^2}\|u - c_i\|_2} \qquad (3)$$

The $\sigma$ parameter determines the width of radial basis function and is commonly known as the expansion parameter. In our case, the expansion parameter of 0.775 was used. Normally, the value of 0.5 is used for the expansion parameter, but for this higher value, we have a better agreement between the measurement value and the simulated data.

A set of 70 samples of measured data was used for training purposes, while the remaining 30 samples were used for testing and simulation purposes. The network training steps consistently regulate the free network parameters (and weights synaptic) based on the mean square error of the predicted values and the measured field strength for a set of random training samples.

$$mse = \frac{1}{N}\sum_{i=1}^{N}(e_i)^2 = \frac{1}{N}\sum_{i=1}^{N}(t_i - a_i)^2 \quad (4)$$

Here, $t_i$ and $a_i$ are the target output and actual output values respectively. When the error between the output of the network and the desired output is minimized, the training process is ended. After the training process, the neural network can be used for testing over the test data.

The main goal of network training is not only to achieve the minimum amount of errors for the training data set, but also the network should be able to work well with data that is not used in the training process. This generalization characteristic is very important in the practical application of the neural model for prediction in environments for which measurement data is not available. The network generalization feature depends on the training samples and training algorithm.

*4.2 Concepts model tree algorithm*

The model tree (MT) is a data-based technique for dealing with continuous class issues which provides a structured data representation and precise linear fit of classes [13]. Also, it is a kind of decision tree that has the ability to predict numeric values with linear regression in leaves and to categorize the data according to their similarity and then matching them with local regression equations, thus helping to reduce the model error. Quinlan and Wang and Witten described these popular techniques [9].

The flowchart of the basic stages of the MT algorithm is shown in Fig. 3, [22]. Initially, the diagram divides the space of the parameter into sub spaces, then generates a linear regression model for each sub space. The diagram uses information theory to divide the data and helps to fit a suitable model. During the formulation of the model, each division section follows the idea of integrity and combination of the decision tree from several models. Finally, the flowchart uses intelligent computing techniques for possible solutions for each model. The main advantages of tree models than regression trees are: (a) Model trees are much smaller than regression trees; (b) The decision-making power is clear; and (c) Regression functions typically do not include many variables. Computational requirements for model trees grow rapidly with dimensions. Hundreds of features are included in the calculations that help to provide better formulas. Tree-based models develop with the division and failure method. Standard deviation reduction (SDR) is the main criterion for choosing a model that is given by the following equation:

$$SDR = sd(T) - \sum_{i}\frac{|T_i|}{T}sd(T_i) \quad (5)$$

In which $T$ represents a set of samples that reaches the node; $T_i$ denotes the subset of samples that result from / * from a potential set (for example, the sets that result from the division of the node based on the selected attribute) and *SD (.)* represents the standard deviation.

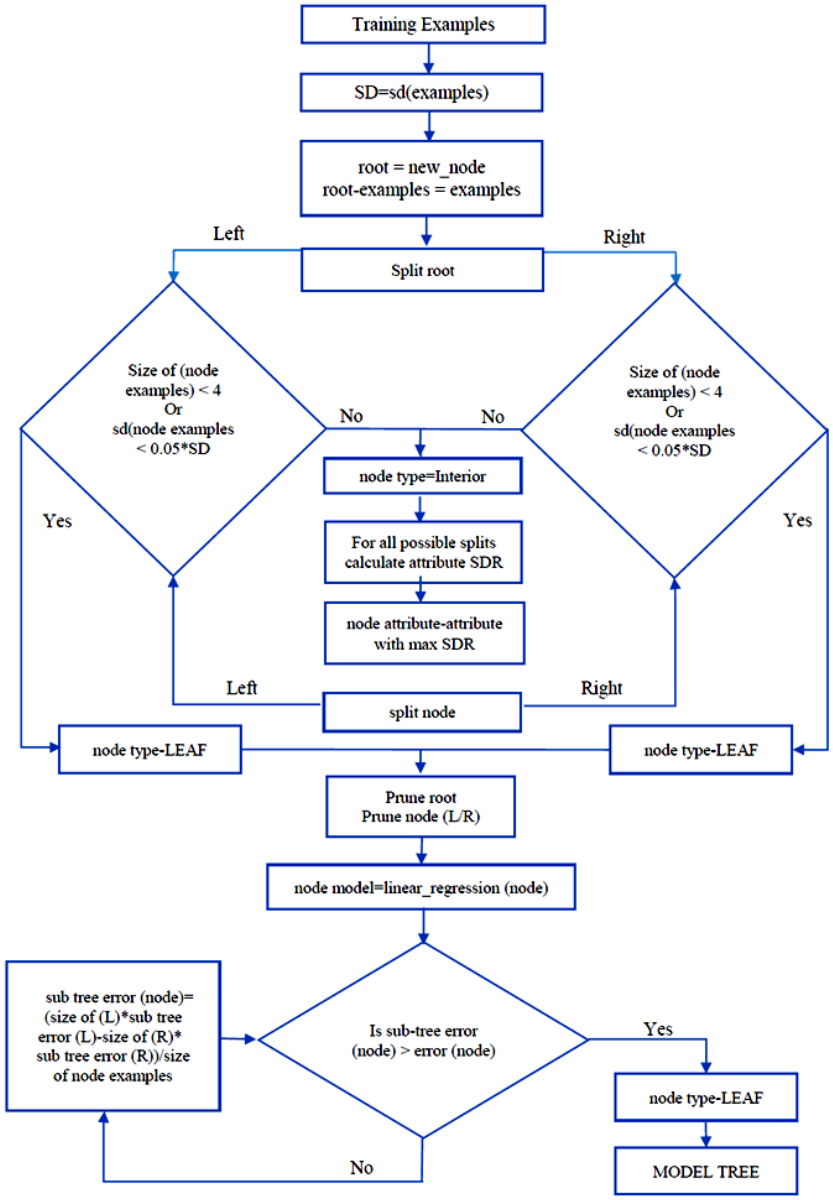


Figure 3. Flow chart of model tree [22]

### *4.2.1 Trimming (pruning) and smoothing model tree*

If the produced trees have more leaves than sufficient leaves, the forecast may be "overly accurate" and too much fit with existing data which will result in poor generalization. It is possible to create a healthier tree by simplifying it. These merging steps are called pruning under the lower trees to a node. The process used to compensate for the extreme difference between adjacent linear models in deciduous tree leaves is called smoothing. Hence, smoothing for models made from a small number of training data is very difficult.

## 5. RESULTS AND DISCUSSION

During the modeling process, the chosen training data set was presented and applied in order to train the considered learning algorithm to radial basis type neural networks (RBF) and the multi-layer perceptron neural networks (feedforward MLP). The purpose of training neural networks is to determine the coefficients of a nonlinear equation that is capable of optimal estimating the test data. The general structure of the radial basis neural network, discussed in this paper, is shown in Fig. 4. The radial basis type neural network uses radial basis functions as activation functions. The output result of this network is usually a linear combination of radial basis functions for input parameters and neurons. The network output is calculated based on a linear function described in equation below:

$$\varphi(x) = \sum_{i=1}^{N} \alpha_i \, \rho(\|x - c_i\| \tag{6}$$

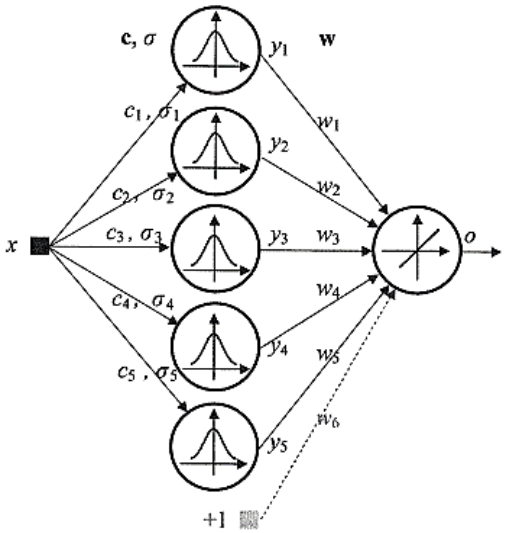


Figure 4. Overall framework of the radial basis neural network

The training algorithm for this network was carried out in two steps. In the first step, the mean vector was calculated for each radial basis function. In the second step, based on a linear function, the coefficients of the hidden layers were selected according to the objective function. The obtained results of the training of the RBF neural network on the training data set in order to predict the bearing capacity of the pile are shown in Fig. 5.

In order to be ensure of achieving the appropriate RBF neural network model, the developed network by testing data set was evaluated. The test data includes information that is not provided to network in the training phase. Fig. 6 shows the evaluation results of the performance of the radial basis function type neural network on the test data.

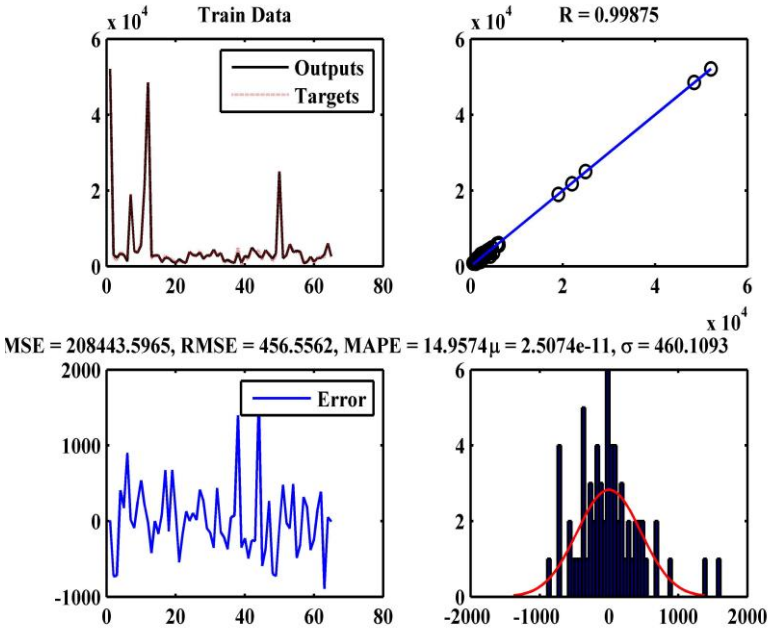


Figure 5. (a) shows the RBF neural network performance based on the training data provided to the RBF neural network (b) shows the regression coefficient calculated based on the training data provided to the RBF neural network (c) indicates the error variation in the performance of the investigating network (d) shows the diagram of the error histogram

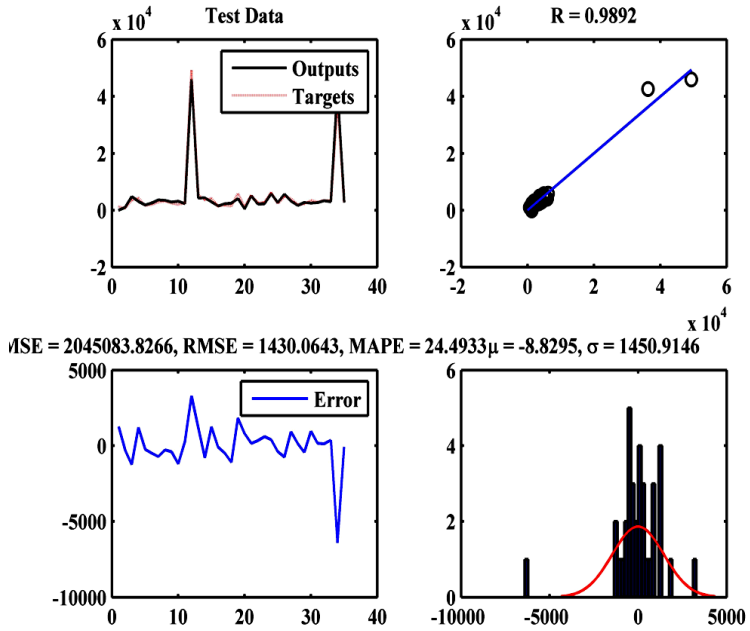


Figure 6. (a) indicates the RBF neural network performance based on the test data set provided to the RBF neural network (b) shows the regression coefficient calculated based on the test data set provided to the RBF neural network (c) indicates the error variation in the performance of the investigating network (d) displays the diagram of the error histogram

In order to evaluate the accuracy of the predicted results with the desired target values and the accuracy of the various used methods, the RBF neural network model was compared with the Multilayer Perceptron Neural Network (MLP) model based on the Levenberg Marquardt (LM) and Bayesian Regulation (BR) learning algorithms and also with tree model (MD). Artificial neural network learning quality evaluation in both training and testing process was obtained by checking general statistical indices such as Root Mean Square Error (RMSE) and Mean Absolute Percentage Error (MAPE) values and Correlation Coefficients.

$$MAPE = \frac{1}{N}\sum_{i=1}^{N}\frac{|A_i - F_i|}{|A_i|}\times 100\% \quad (7)$$

$$RMSE = \sqrt{\frac{1}{N}\sum_{i=1}^{N}[A_i - F_i]^2} \quad (8)$$

where $N$ is number of predictions, $A_i$ and $F_i$ are predicted values and actual values respectively. MAPE is one of the criteria of the error percentage that are popular and one of the most widely used standards without units. The results of this evaluation for the training dataset and testing dataset are shown in Table 3 and Table 4 respectively for different applied methods in this study.

Table 3: Results of the evaluation in training stage for various methods

| Methods | MAPE | RMSE | Correlation |
|---|---|---|---|
| RBF | 14.95 | 456.55 | 0.99875 |
| MLP_LM | 22.08 | 2994.47 | 0.93819 |
| MLP_BR | 34.04 | 1171.4806 | 0.99077 |
| MODEL TREE | 30.23 | 2602.14 | 0.94102 |

Table 4: Results of evaluation in testing stage for various methods

| Methods | MAPE | RMSE | Correlation |
|---|---|---|---|
| RBF | 24.49 | 1430.06 | 0.9892 |
| MLP_LM | 32.06 | 4837.52 | 0.93032 |
| MLP_BR | 39.35 | 1647.05 | 0.9849 |
| MODEL TREE | 50.61 | 4248.23 | 0.97395 |

As it can be seen, most of the networks have a high correlation coefficient. However, the radial basis neural network (RBF) is the highest amount of correlation coefficients. Compared to ANNs, RBF network is a better answer. Training dataset and testing dataset have been assigned to values of R = 0.99875, RMSE = 456.55, R = 0.9892 and RMSE = 1430.06 respectively. The other networks which despite the high correlation coefficient, have a high error in training and testing of their network. The most common networks such as MLP with simpler structure will significantly decrease network error in case of eliminating some input parameters and even separation of adhesive soil and granular ones.

However, with many input parameters, RBF has considered more effective artificial neural network system to approximate the ultimate bearing capacity of the single piles. Correlation coefficient charts of mentioned methods together with proposed RBF neural network has been shown in Fig. 7.

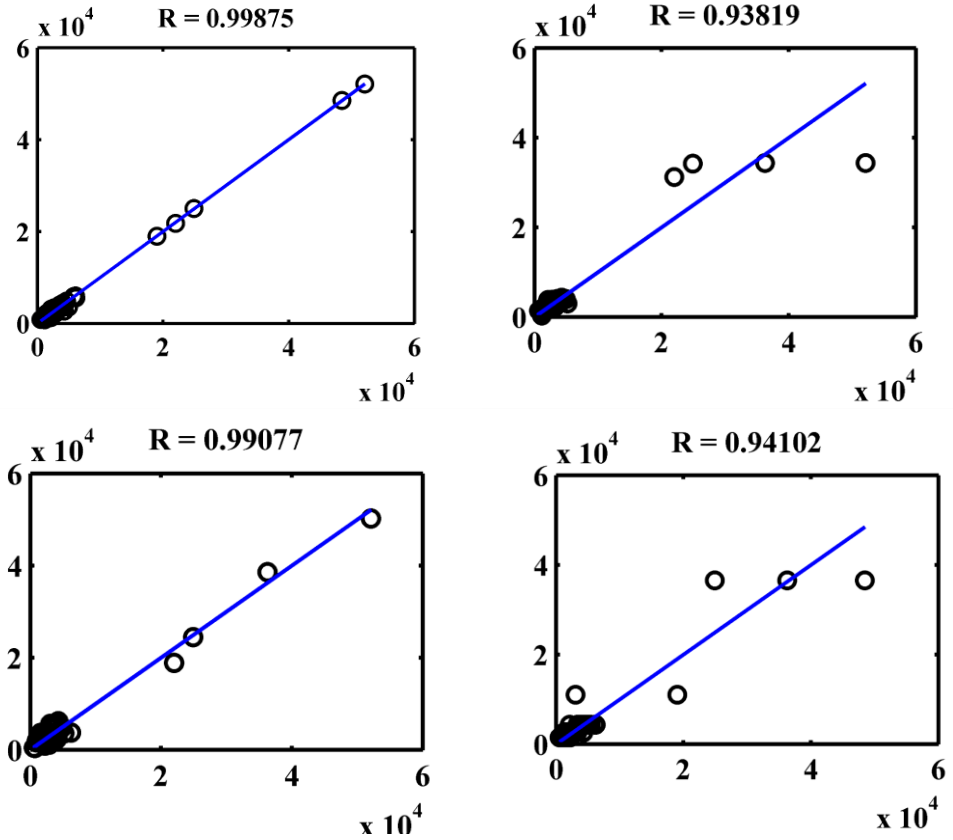


Figure 7. (a) Radial Basis Function Type Neural Network (b) Multilayer Perceptron Neural Network with Levenberg-Marquardt Backpropagation Training Algorithm (c) Multilayer Perceptron Neural Network with Bayesian Regulation Backpropagation Training Algorithm (d) Model Tree Algorithm

## 6. CONCLUSION

In this research, various neural networks have been developed to calculate and predict the ultimate axial bearing capacity of single piles on a database collected from existing papers consisting of 100 prefabricated concrete and steel piles that were presented at the time of the publication of this study. Always by increasing the training process of neural networks, it is not expected that the developed network will show a lower error in its output estimation because the investigating network may be over-trained and learned only training data and does not respond to not provided test data to the network. In general, in this study, we concluded that the radial basis neural network (RBF) yielded a response approximately close

to the target value and achieves results with less than 10% of the mean absolute error for the test data set compared to other used methods. With providing the required information in order to present to developed neural network and training of the neural network using the used algorithms, It was concluded that the use of trained neural network techniques was much simpler than the numerical and empirical methods used to estimate and analyze the ultimate bearing capacity of piles. It was observed that multi-layer perceptron neural network error is high due to the number of input data but by decreasing the number of network input parameters and changing the structure of the investigating network, we can reduce the error of multilayer perceptron neural networks. However, due to the number of input parameters (Table 2) and the results of various methods used in this study, it was determined that the radial basis type neural network has better performance and efficiency than the methods used to estimate the bearing capacity of the piles with approximation close to target values.

## REFERENCES


1. Goh AT. Empirical design in geotechnics using neural networks, *Geotech* 1995; **45**(4): 709-14.
2. Goh ATC. Pile driving records reanalyzed using neural networks, *J Geotech Eng* 1996; **122**(6): 492-5.
3. Lee IM, Lee JH, Prediction of pile bearing capacity using artificial neural networks, *Comput Geotech* 1996; **18**(3): 189-200.
4. Teh C, Wong KS, Goh AT, Jaritngam S. Prediction of pile capacity using neural networks, *J Comput Civil Eng* 1997; **11**(2): 129-38.
5. Kiefa MA. General regression neural networks for driven piles in cohesionless soils, *J Geotech Geoenvironm Eng* 1998; **124**(12): 1177-85.
6. Hanna AM, Morcous G, Helmy M. Efficiency of pile groups installed in cohesionless soil using artificial neural networks, *Canad Geotech J* 2004; **41**(6): 1241-9.
7. Shahin MA, Jaksa MB, Maier HR. Recent advances and future challenges for artificial neural systems in geotechnical engineering applications, *Adv Artific Neural Syst* 2009; **2009**: 5.
8. Najafzadeh M, Barani GA. Comparison of group method of data handling based genetic programming and back propagation systems to predict scour depth around bridge piers, *Scientia Iranica* 2011; **18**(6): 1207-13.
9. Najafzadeh M, Laucelli DB, Zahiri A. Application of model tree and evolutionary polynomial regression for evaluation of sediment transport in pipes, *KSCE J Civ Eng* 2017; **21**(5): 1956–63.
10. Kordjezi A. pooyanejad F. Predicting the bearing capacity of piles using support vector machine based on CPT data, 2013, Mashhad, Iran.
11. Maizir H, Kassim KA. Neural network application in prediction of axial bearing capacity of driven piles, *in Proceedings of the International MultiConference of Engineers and Computer Scientists*, IMECS, Hong Kong, 2013.
12. McVay MC, Klammler H, Tran K. Pile/Shaft Designs Using Artificial Neural Networks (ie, Genetic Programming) with Spatial Variability Considerations, 2014.

13. Najafzadeh M, Barani GA, Hessami-Kermani MR. Group method of data handling to predict scour depth around vertical piles under regular waves, *Scientia Iranica* 2013; **20**(3): 406-13.
14. Najafzadeh M, Barani GA, Hessami-Kermani MR. Evaluation of GMDH networks for prediction of local scour depth at bridge abutments in coarse sediments with thinly armored beds, *Ocean Eng* 2015; **104**, 387-96.
15. Kaveh A, Fazel-Dehkordi D, Servati H. Prediction of moment-rotation characteristic for saddle-like connections using FEM and BP neural networks, *In: International Conference on Engineering Computational Technology* 2000; pp. 15–24.
16. Kaveh A, Raeisi Dehkordi M. Neural networks for the analysis and design of domes, *Int J Sp Struct* 2003; **18**(3): 181–93.
17. Kaveh A, Iranmanesh A. Comparative study of backpropagation and improved counterpropagation neural nets in structural analysis and optimization, *Int J Sp Struct* 1998; **13**(4): 177–85.
18. Kaveh A, Servati H. Design of double layer grids using backpropagation neural networks. Comput Struct 2001; **79**(17): 1561-8.
19. Kaveh A, Elmieh R, Servati H. Prediction of moment-rotation characteristic for semi-rigid connections using BP neural networks, 2001.
20. Kaveh A, Raeisi DM. Application of artificial neural networks for predicting the displacements of domes under wind loading, 2007.
21. Milad F, Kamal T, Nader H, Erman OE. New method for predicting the ultimate bearing capacity of driven piles by using Flap number, *KSCE J Civ Eng* 2015; **19**(3): 611–20.
22. Janga Reddy M, Ghimire BNS. Use of model tree and gene expression programming to predict the suspended sediment Load in rivers, *J Intell Syst* 2009; **18**(3): 211–27. Available from: http://www.scopus.com/inward/record.url?eid=2-s2.0-71549155647&partnerID=40&md5=85626306e79226bb9e7380cb8ea745af.